Compact 10 GHz loopback arrayed-waveguide grating for high-fidelity optical arbitrary waveform generation

Nicolas K. Fontaine,[1,*] Ryan P. Scott,[1] Chunxin Yang,[2] David J. Geisler,[1] Jonathan P. Heritage,[1] Katsu Okamoto,[1] and S. J. B. Yoo[1]

[1]*Department of Electrical and Computer Engineering, University of California, Davis, California 95616, USA*
[2]*Department of Applied Science, University of California, Davis, California 95616, USA*
[*]*Corresponding author: nkfontaine@ucdavis.edu*

Received April 9, 2008; revised June 17, 2008; accepted June 19, 2008;
posted June 27, 2008 (Doc. ID 94849); published July 25, 2008

We demonstrate a high-performance optical arbitrary waveform shaper based on a single 10 GHz arrayed-waveguide grating with 64 loopback waveguides and integrated amplitude and phase modulators on each waveguide. The design is compact and self-aligning and allows for bidirectional operation. The device's complex transfer function is manipulated and measured over the full 640 GHz passband. To demonstrate optical arbitrary waveform shaping, high-fidelity 15-line shaped waveforms are measured with cross-correlation frequency-resolved optical gating. © 2008 Optical Society of America

OCIS codes: 080.1238, 320.5540, 320.7100, 120.5050, 320.7160.

Optical arbitrary waveform generation (OAWG) offers solutions for applications where complete control of light, both amplitude and phase, with tremendous bandwidth is required. Such applications include generation of ultrahigh-bandwidth communication signals and arbitrarily shaped pulses for molecular probing [1]. OAWG can be accomplished via many methods, either in the time domain, the Fourier domain, or a combination of both, as long as the amplitude and the phase of the waveform can be fully specified for a particular bandwidth and duration.

The loopback arrayed-waveguide grating (AWG) based waveform shaper (WS) described in this Letter performs OAWG via line-by-line Fourier synthesis by exactly replicating the desired waveform's complex spectrum (amplitude and phase) [1–3]. This differs from conventional pulse shaping, where groups of lines are manipulated [4]. Figure 1(a) illustrates Fourier synthesis by applying dc amplitude and phase modulation to each line (mode) of an optical frequency comb (OFC) using a Fourier domain WS. In the WS, a spectral demultiplexer isolates the individual frequencies to discrete spatial locations where modulators shape each line separately. Then a multiplexer combines the frequencies at different spatial locations to a single output. The OFC (i.e., input waveform) is a repetitive temporal waveform with a period T and a spectrum consisting of individual comb lines spaced by the repetition rate. Therefore the maximum length of a shaped waveform is limited to T. The appeal of Fourier synthesis is its ability to generate very short temporal features; the temporal resolution, or shortest waveform feature, is proportional to the inverse of the total bandwidth of the OFC. Extending the duration of the waveforms is difficult, because the OFC's comb spacing must be reduced, which forces a higher spectral resolution requirement on the WS. Previously demonstrated dispersive elements such as AWGs, virtually imaged phase arrays, or diffraction-grating-based pulse shapers do not easily resolve significantly below 1 GHz (i.e., >1 ns waveform duration) while maintaining a large bandwidth [1,5]. The resolution requirement can be circumvented by using high-speed phase and amplitude modulators with bandwidths equal to the resolution of WS rather than using dc modulation. AWG-based WSs can be implemented as compact, fiber-coupled integrated devices in silica, indium-phosphide, or silicon technologies, a key requirement for OAWG to find widespread application. Additionally, using the indium-phosphide or silicon platforms it is possible to achieve greater than 1 GHz modulation bandwidths [6]. Selecting a common bandwidth between 5 and 40 GHz is a compromise between high optical resolution and high electrical modulation rate limitations. Increasing the optical resolution always requires an increase in the size of the AWG. At some point, the larger AWGs are extremely susceptible to refractive index nonuniformities and as a result have distorted filtering functions. This leads to spectral misalignment between the two AWGs in an AWG-pair WS [Fig. 1(a)]. Self-matched

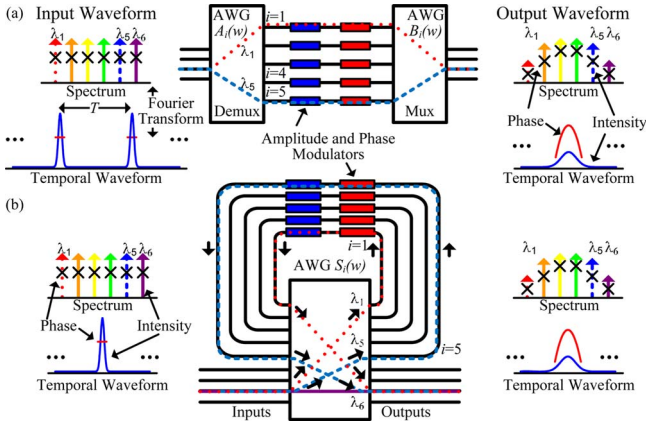

Fig. 1. (Color online) (a) Depiction of an AWG-pair waveform shaper and (b) a loopback AWG waveform shaper. Dashed spectral lines follow paths as shown.

0146-9592/08/151714-3/$15.00

reflective-mode AWG-pair geometries have been demonstrated as WSs [7]; however they are not unidirectional and therefore should not be used with broadband modulators integrated onto each wavelength channel. To overcome these limitations, we developed a novel loopback AWG WS design [Fig. 1(b)] to replace a high-speed AWG-pair WS. Our design significantly reduces the device size and avoids the difficulties of fabricating two identical AWGs. In this Letter, we expand upon [8] and fully describe a 64 loopback waveguide (i.e., 64 channel), 10 GHz, 1 THz free-spectral-range (FSR) AWG WS with four input–output pairs. Measurement of the complex transfer function and shaping of two waveforms show its use as a high-fidelity WS.

As mentioned previously, Fig. 1(a) shows an AWG-pair WS where $A_i(\omega)$ and $B_i(\omega)$ describe demultiplexing transmission from either the input to output i for a demultiplexer or from input i to the output for a multiplexer. The input AWG separates the wavelengths, the modulator array provides modulation, and the output AWG combines the wavelengths. Figure 1(b) shows how a loopback AWG performs the same operation, since $A_i(\omega)$ and $B_i(\omega)$ are both described by $S_i(\omega)$. The operation of the device can be illustrated by tracing a single wavelength through the WS schematic (represented by dashed lines). The AWG demultiplexes λ_1 on the input to the inner loopback waveguide, where Mach–Zehnder modulators (MZMs) and phase modulators (PMs) provide amplitude and phase modulation. The loopback waveguide then directs λ_1 to an input of the AWG. Symmetric fabrication of the input and output coupler of the AWG force this wavelength to be directed toward an output. Likewise, the AWG will demultiplex λ_5 to the outer loopback waveguide, the modulators apply modulation, and the AWG will multiplex λ_5 back to the output. One wavelength λ_6 is demultiplexed directly to the output, bypassing the loopback arms. Both the AWG-pair WS and loopback AWG WS provide cascaded filtering of $A_i(\omega)\times B_i(\omega)$ or $S_i(\omega)\times S_i(\omega)$ to reduce crosstalk. Generally, with a loopback AWG WS, a portion of the signal during its first pass through the AWG increases the crosstalk. However, this crosstalk is suppressed by inserting a half-wave plate in the center of the AWG [see Fig. 2(a)]. The signal traveling through the AWG once (i.e., AWG-only response) will be on an orthogonal polarization to the signal traveling through the AWG twice (i.e., WS response) and can be removed with a polarizer. Some advantages of the loopback AWG design are decreased wafer size, identical multiplexing and demultiplexing operations, and simplified fabrication and error correction. Additionally, the optical signals travel unidirectionally through each modulator, allowing future devices to incorporate high-speed traveling-wave modulators. Both the MZMs and PMs use 10-mm-long, chromium-based resistive heaters to obtain phase shifts via the thermo-optic effect. Trenches are used to concentrate the heating to a single waveguide and reduce crosstalk between adjacent modulators. Figure 2(a) depicts the layout of the fabricated WS as it is used in the waveform shaping

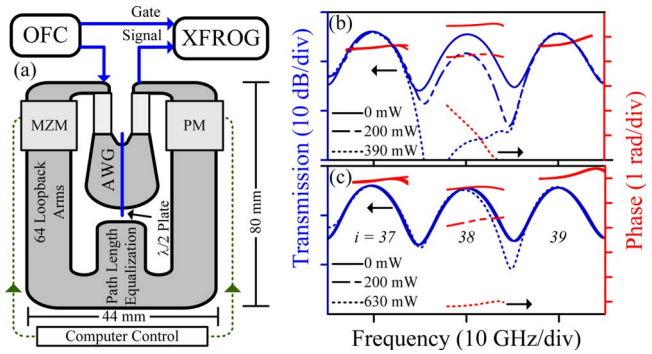

Fig. 2. (Color online) (a) OAWG waveform shaping experimental arrangement. WS transmission for three channels with different electrical powers applied to channel 38's (b) MZM and (c) PM (amplitude in black and phase in gray).

experiment. Figure 2(b) is the complex transfer function of three adjacent loopback waveguides ($i=37-39$) in the WS when electrical power is applied to a single MZM. Greater than 20 dB of extinction is attained at 390 mW with some associated phase shift (MZM is not push–pull). Figure 2(c) shows electrical power applied to a single PM. At 630 mW, 5.5 rad of phase modulation is achieved with little amplitude modulation. The data indicate the WS resolves spectral lines spaced at 10 GHz.

Measurements of the complex optical transmission and time-domain impulse response of the loopback AWG WS are performed using a frequency-domain interferometer [9]. Figure 3(a) shows the full transmission of the AWG, $S_{68}(\omega)$, on the same and orthogonal polarization when compared to the WS response ($\Sigma_{i=1}^{64} S_i(\omega)\times S_i(\omega)$). The WS transmission is flat because it spans 640 GHz of the 1 THz AWG FSR. Figure 3(b) shows the AWG impulse response, and Fig. 3(c) presents the WS impulse response (1.5 ns later), each on an orthogonal polarization. The WS's crosstalk can be determined by temporally filtering the AWG and WS responses on the WS's polarization and viewing the filtered response in the frequency domain [Fig. 3(a)]. The crosstalk suppression is >40 dB. Each sample in Fig. 3(b) corresponds to the phase and amplitude transmission of an individual arrayed waveguide (280 total). Flattening the phase across all arms would improve the transmission of the AWG in a process known as AWG phase-error correction. Figure 3(d) shows the WS response with no power to the MZMs or PMs. Figure 3(e) presents the result after flattening the phase and amplitude response of each channel. The imperfect flattening of the phase on a few channels is caused by the electronic driving circuit's maximum output of 630 mW, short of the 780 mW needed to achieve a 2π phase shift (heater is rated at 1 W). Figure 3(c) shows the impulse response of the uncorrected transmission [Fig. 3(d)] and corrected transmission [Fig. 3(e)]. The features at ±100 ps from the center are due to periodic filtering in the frequency domain.

Referring back to Fig. 2(a), in the OAWG shaping experiment the WS is used to shape a 15 lines of a 10 GHz OFC into two different target waveforms. Precision computer control sets the phase of the PMs

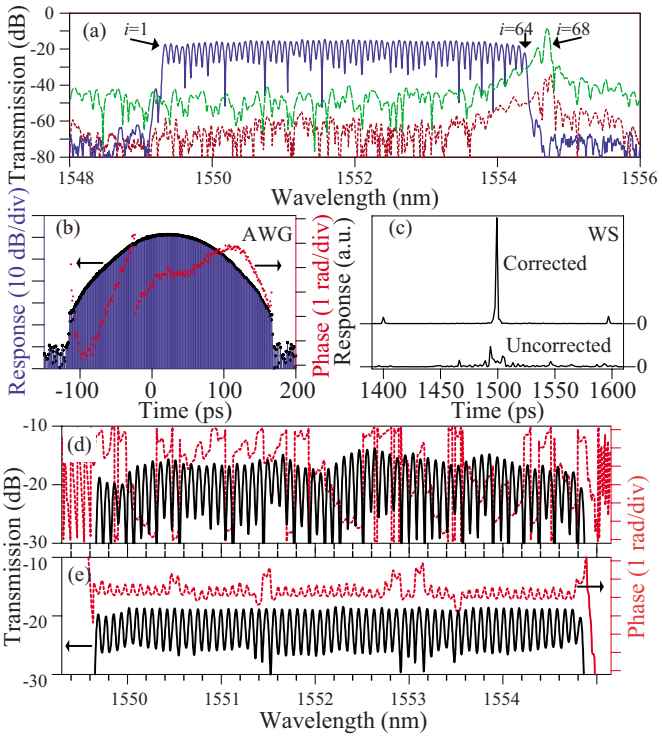

Fig. 3. (Color online) (a) Transmission of AWG (long dashed curve), WS (solid curve), and AWG on WS polarization (short dashed curve). Impulse response of (b) AWG. (c) Energy normalized impulse response of WS. Intensity (solid curve) and phase (dotted curve) transmission of waveform shaper (d) without correction and (e) with phase and intensity flattening.

with milliradian resolution. Cross-correlation frequency-resolved optical gating (XFROG) [2,10] fully characterizes the shaped waveforms. The OFC is a repetitive 100 ps pulse train with 7 ps pulsewidth. The OFC and WS can create any repetitive waveform with a duration of 100 ps and a bandwidth of 150 GHz, although the WS can support up to 640 GHz. The XFROG uses the OFC as a reference waveform to measure an unknown waveform. Performance of the OAWG system is measured using G' (G prime) as a figure-of-merit [11]. G' is the rms difference between the FROG traces generated from the target and shaped waveforms, normalized to the target FROG trace energy. This is similar to the FROG retrieval error parameter G [10]. In one number, G' provides a clear indication of how closely the shaped waveform matches the target waveform in both intensity and phase and in both temporal and spectral domains. A G' lower than 5% represents a high-fidelity waveform that is an excellent match to the target. Typically 5–10 iterations of measurement and correction are required to achieve $G' < 5\%$ because of crosstalk sources, including electrical, optical, and nonuniform device heating. Figures 4(a)–4(c) show a shaped waveform with pure quadratic spectral phase (QSP), which is equivalent to the linear dispersion of 1.4 km of single-mode fiber. Figures 4(d)–4(f) show a pulse shaped to have flat spectral phase. The spectral intensity of both waveforms is shaped to a sixth-order super Gaussian. G' of 4.9% and 2% were obtained for the QSP waveform and transform-limited waveform, respectively. The spectral phase errors between the target and measured waveforms are less than ±0.02 rad per mode. It is important to note that the larger G' for the QSP waveform does not indicate inferior waveform shaping. Rather, it merely emphasizes that waveforms occupying the entire temporal window are sensitive to small shaping errors.

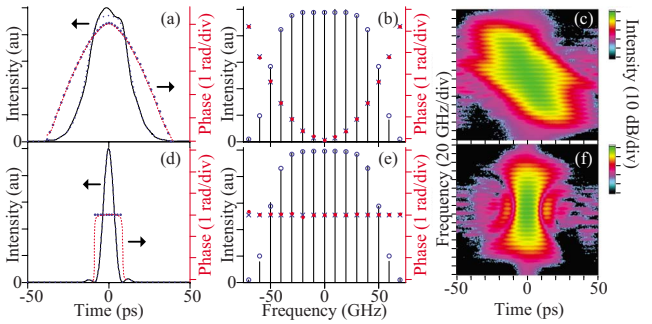

Fig. 4. (Color online) (a)–(c) QSP waveform. (d)–(f) Transform-limited waveform. (a), (d) Time domain; (b), (e) spectral domain; (c), (f) XFROG trace. Measured waveforms intensity (solid curve, squares); phase (dashed curve, closed circles); target waveforms (dotted curve, open circles, x).

We have presented a novel 64-channel, 10 GHz high-resolution loopback AWG WS with amplitude modulators and phase modulators on each loopback arm. The loopback AWG design self-aligns the spectral demultiplexing and multiplexing operation of the WS, a critical requirement for a high-resolution WS. On the basis of the success of this proof-of-principle, future work will proceed toward implementing the design in InP technology.

This work was supported in part by the DARPA DSO and SPAWAR under OAWG contract HR0011-05-C-0155.

References

1. Z. Jiang, C.-B. Huang, D. E. Leaird, and A. M. Weiner, Nat. Photonics **1**, 463 (2007).
2. N. K. Fontaine, R. P. Scott, J. Cao, A. Karalar, K. Okamoto, J. P. Heritage, B. H. Kolner, and S. J. B. Yoo, Opt. Lett. **32**, 865 (2007).
3. K. Takiguchi, K. Okamoto, T. Kominato, H. Takahashi, and T. Shibata, Electron. Lett. **40**, 537 (2004).
4. A. M. Weiner, Prog. Quantum Electron. **19**, 161 (1995).
5. K. Takada, M. Abe, T. Shibata, and K. Okamoto, J. Lightwave Technol. **20**, 850 (2002).
6. N. Kikuchi, K. Tsuzuki, E. Yamada, H. Yasaka, and T. Ishibashi, Proc. SPIE **6014**, 601409-1 (2005).
7. K. Mandai, D. Miyamoto, T. Suzuki, H. Tsuda, K. Aizawa, and T. Kurokawa, IEEE Photonics Technol. Lett. **18**, 679 (2006).
8. N. K. Fontaine, D. J. Geisler, R. P. Scott, C. Yang, F. M. Soares, A. Karalar, J. Yang, K. Okamoto, J. P. Heritage, and S. J. B. Yoo, in *Optical Fiber Communication Conference*, OSA Technical Digest (CD) (Optical Society of America, 2008), paper OTuC7.
9. K. Takada and S.-I. Satoh, Opt. Lett. **31**, 323 (2006).
10. R. Trebino, *Frequency-Resolved Optical Gating: The Measurement of Ultrashort Laser Pulses* (Kluwer, 2002).
11. R. P. Scott, N. K. Fontaine, J. Cao, K. Okamoto, B. H. Kolner, J. P. Heritage, and S. J. B. Yoo, Opt. Express **15**, 9977 (2007).